

Effect of molecular weight of PEG on membrane morphology and transport properties

B. Chakrabarty, A.K. Ghoshal^{*}, M.K. Purkait^{*}

Department of Chemical Engineering, Indian Institute of Technology Guwahati, Guwahati 781039, India

Received 14 August 2007; received in revised form 16 October 2007; accepted 20 October 2007

Available online 26 October 2007

Abstract

Flat sheet asymmetric polymeric membranes were prepared from homogeneous solution of polysulfone (PSf) by phase inversion method. *N*-methyl-2-pyrrolidone (NMP) and dimethyl acetamide (DMAc) were used as solvents separately. Polyethylene glycol (PEG) of three different molecular weights (400 Da, 6000 Da and 20000 Da, respectively) were used as the polymeric additives in the casting solution. The morphology and structure of the resulting membranes were observed by scanning electron microscope (SEM). The pore number, pore permeability and their distribution and average pore size of the membranes were determined by the liquid displacement method. The permeation performances of the membranes were evaluated in terms of pure water flux (PWF), equilibrium water content (EWC), hydraulic permeability, and solute rejection. Solution of bovine serum albumin (BSA) of molecular weight 68,000 Da was used to study the permeation performance of prepared membranes using a batch membrane cell of 100 mL capacity. Results showed that with increase in molecular weight of PEG, the pore number as well as pore area in membranes increases. Membranes with PEG of higher molecular weights have higher PWF and higher hydraulic permeability due to high porosity. With increase in molecular weight of PEG from 400 to 20000, the PWF increases from 15.3 to 2713.4 L m⁻² h⁻¹ with NMP as solvent while with DMAc as solvent, the PWF increases from 24.5 to 555.6 L m⁻² h⁻¹. Similarly, EWC increases from 56.8% for PEG 400 to 78.8% for PEG 20000 for PSf/NMP/PEG membranes. Similar trend is observed for PSf/DMAc/PEG membranes. The BSA rejection data is maximum with PEG 6000 for both the solvents and the values are 56.4% for NMP (at pH 4.8) and 42.4% for DMAc (at pH 9.5).

© 2007 Elsevier B.V. All rights reserved.

Keywords: Polysulfone membrane; Phase inversion method; Polyethylene glycol; Scanning electron microscopy; Protein rejection

1. Introduction

Phase inversion is one of the most important processes for preparing both symmetric and asymmetric polymeric membranes. The structure of phase inversion membranes results from a phase change of initially stable polymer solutions. These membranes are widely used today in various applications such as microfiltration, ultrafiltration, reverse osmosis and as supports for composite structures [1,2]. It is actually a diffusion-induced phase separation process, which involves conversion of a liquid polymer solution of two or more components into a two-phase system, like; solid polymer rich phase and the liquid polymer poor phase. The solid phase forms the membrane structure while

the liquid phase forms the membrane pores. The conversion is generally carried out by addition of a precipitating fluid which is usually miscible with the solvent but immiscible with the polymer. The mechanism of formation of these membranes has been the subject of investigation since many years. Reuvers et al. [3] developed a model which describes the mass transfer phenomena occurring during the immersion step. The model explained the two types of demixing taking place during the phase inversion process, i.e. instantaneous demixing and delayed demixing. Membranes formed by instantaneous demixing generally show a highly porous substructure (with macrovoids) and a finely porous, thin skin layer. Membranes formed by a delayed demixing mechanism show a porous (often closed-cell, macrovoid-free) substructure with a dense, relatively thick skin layer. Structure and properties of membranes prepared by phase inversion method depend upon many factors. Addition of additive into the casting solution is one of the major factors. An additive is used in the casting solution in order to have an opti-

^{*} Corresponding author. Tel.: +91 361 2582262; fax: +91 361 2582291.

E-mail addresses: aloke@iitg.ernet.in (A.K. Ghoshal), mihir@iitg.ernet.in (M.K. Purkait).

mal membrane structure. The additive can be a single component or a mixture. Generally the additive being a weak non-solvent for the polymer, reduces the solvent power in the solution. A number of researchers [4–7] have reported their observation on the role of additives in the membrane structures. Well known additives are glycerol in a system of polysulfone (PSf)/dimethyl acetamide (DMAc)/water, maleic acid in a system of cellulose acetate/dioxane/water, polyvinyl pyrrolidone (PVP) in a system of PSf/*N*-methyl-2-pyrrolidone (NMP)/water, polyethylene glycol (PEG) in polyvinylidene difluoride (PVDF)/dimethyl formamide (DMF) or (DMAc)/water system, etc. [4]. Either enlargement or suppression of macrovoid can be obtained using the same additive, but with a variation of additive concentration or additive molecular weight. While some additives have the tendency to form macrovoids, others help in suppressing the macrovoids improving interconnectivity of the pores and resulting in higher porosities in the top layer and the sub layer. Boom et al. [4] studied the role of PVP as polymeric additive in the formation of the membrane with poly (ether sulfone) (PES) in NMP as solvent and found that the addition of PVP suppresses the formation of macrovoids by reducing the possibility of delayed demixing. Wienk et al. [5] investigated the effects of addition of a high and low molecular weight component to the casting solution. They proposed a mechanism for the formation of nodular structures in the top layer of membrane. Jimenez et al. [6] studied the effect of PVP as additive on PES membranes and showed that the addition of PVP increased the molecular weight cut off (MWCO) and pure water permeation of the PES membranes. Yeo et al. [7] found that PVP addition to the casting solution of PSf and DMF, contributes to the enlargement of the macrovoid structure in the prepared membranes rather than the suppression of that structure. Jung et al. [8] from their study on the effect of molecular weight of polymeric additives, PVP, on the morphology and water flux of polyacrylonitrile (PAN) concluded that the top layer of the membrane and suppression of macrovoid formation strongly depend upon the molecular weight of PVP. Han and Nam [9] reported the effect of PVP introduction on the thermodynamic and rheological properties in PSf casting solution. Han [10] showed that the number of the polymer aggregates or of the nucleation sites is increased by the addition of propionic acid (PA) into PSf casting solution. Ping et al. [11] studied the interaction between polysulfone (PS) and 71 low molecular weight organic compounds with different functional groups by the gas liquid chromatography (GLC) and proposed a model to explain the experimental results. Zheng et al. [12] in their recent work described the effect of rheological and thermodynamic variation of PSf casting solution due to PEG introduction on the kinetics of membrane formation. The effects of PEG concentrations on the porosity of polycarbonate (PC) membranes prepared via dry/wet-phase inversion methods was studied by Deniz [13]. Chaturvedi et al. [14] have studied the effect of natural additives such as maleic acid and piperazine on performance of PES ultrafiltration membranes. Other researchers studied the effect of different molecular weight PVP such as PVP K10, PVP K30, PVP K90 and PVP K360 on performance of PES membranes [15–17]. Kim and Lee [18] investigated the effect of various molecular weights of PEG on the formation of polyetherim-

ide (PEI) asymmetric membrane and they reported that small molecular weights of PEG such as PEG 200 and PEG 400 work as pore reducing agent for PEI membranes. PEG with molecular weight of 600 Da, 2000 Da, 6000 Da and 12,000 Da was used as additives to control the thermodynamics and kinetics in casting solution of PSf membranes in Kim and Lee's work [19]. Shieh et al. [20] reported that PEG being hydrophilic in nature, is used to improve membrane selectivity as well as a pore forming agent. Idris et al. [21] found that presence of PEG of different molecular weights exhibit significant effect on performance of PES membranes. From the above literatures, although it appears that a number of works has been reported using PEG as additives, there is yet no report regarding the effect of PEG 400, PEG 6000 and PEG 20000 on morphology and performance of PSf membranes. In view of this, an attempt is made to investigate the effect of adding PEG of wide range of molecular weights viz. 400 Da, 6000 Da and 20,000 Da as additives into PSf membranes.

In the present work, the variations of the morphology and the structure of the PSf prepared by diffusion induced phase separation process are reported. PEG of three different molecular weights (400 Da, 6000 Da and 20,000 Da) were used as additives, separately. Two different solvents like, NMP and DMAc were used to prepare PSf membrane. Effects of molecular weight of additive (PEG) and the nature of solvent (DMAc and NMP) on morphology and the permeation characteristics of the prepared membrane were investigated in detail. Morphology of each membrane was analyzed by scanning electron microscopy (SEM). Liquid displacement method was used for studying the parameters related to membrane morphology. Finally, the performance of the membranes was investigated by water permeation and protein (BSA) rejection behaviour.

2. Experimental

2.1. Materials

PSf (average molecular weight 30,000 Da) supplied by Sigma-Aldrich Co., USA, was used as the base polymer in the membrane casting solution. Reagent grade NMP (99.5% purity) and DMAc (99% purity) were used as solvents. Both the solvents were supplied by Central Drug House (CDH) Ltd., India and used without further purification. Reagent grade PEG (average molecular weight 400 Da, 6000 Da and 20000 Da) were used as the non-solvent pore forming additives in the casting solution. Deionized water purified with Millipore system (Millipore, France) was used as the main non-solvent in the coagulation bath. Bovine serum albumin (BSA) with molecular weight of 68,000 Da was obtained from CDH Ltd., India.

2.2. Membrane preparation

Flat sheet PSf membranes were prepared by phase inversion method. Measured amount of polymer (PSf) was dissolved in the two solvents viz. NMP and DMAc, separately at room temperature ($\approx 25^\circ\text{C}$) and relative humidity ($\approx 72\%$). Each solvent mixture was then mixed with 5 wt% of PEG (400 Da, 6000 Da and 20000 Da), separately to make the casting solution. Mem-

Table 1
Composition of the casting solution

Membranes	Additives (wt%)			Solvent (wt%)	
	PEG 400	PEG 6000	PEG 20000	NMP	DMAc
PSf1	5	–	–	83	–
PSf2	–	5	–	83	–
PSf3	–	–	5	83	–
PSf4	5	–	–	–	83
PSf5	–	5	–	–	83
PSf6	–	–	5	–	83

PSf: 12 wt%.

branes with different composition were designated as PSf1, PSf2, PSf3, PSf4, PSf5 and PSf6. Table 1 represents the composition of different membranes. The polymer (PSf) concentration was kept constant at 12%, keeping the solvent and additive concentration at 88%. The polymer solution was stirred for about 6 h at room temperature using a magnetic stirrer. When the solution (consisting of polymer, solvent and the additive) became homogeneous, it was kept at room temperature for 24 h. Subsequently, the solution was spread uniformly on a glass plate (0.01 m × 0.01 m) with the help of a casting knife maintaining a clearance of approximately 0.3 mm between the knife and the plate. The resulting film was then exposed for about 30 s to ambient before immersion into coagulation bath containing water at room temperature. The casted films changed their color from transparent to white immediately after immersion into the coagulation bath and separates out of the glass plate after some time. The prepared membrane sheets were washed under running water to remove the additional amount of additive and then kept overnight in a deionized water bath. Finally, the sheets were air dried at room temperature after cutting them into the form of circular disks of diameter 0.03 m to place inside the membrane cell for filtration experiments.

2.3. Membrane characterization

The shape and size of the pores as well as pore size distribution and porosity are important parameters deciding the separation performance [22]. Membranes so prepared were characterized by morphological analysis and permeation experiments. The morphology of the prepared membranes was investigated by microscopic observations and performing liquid displacement tests. The performance of all the membranes were evaluated in terms of their pure water flux, equilibrium water content, permeate flux as well as percentage of BSA rejection with the help of permeation experiments in batch mode of operation.

2.3.1. Morphological studies

2.3.1.1. Microscopic observation. Microscopic observation was carried out by a scanning electron microscope (LEO 1430VP, UK) which directly provides the visual information of the top surface as well as cross-sectional morphology of the membranes. Computerized analysis of SEM image is a standard and widely used method for the investigation of perforated

materials [23,24]. However, in the present study, the morphological parameters such as pore size, pore number, etc could not be measured from the SEM photographs as almost all the pores are in the ultrafiltration range. Such practice would only give rough approximation of the pore size by overestimating the smallest pores on the surface and also by considering dead end (blocked) pores along with the open pores [1]. Liquid displacement method was adopted to compare the morphology of different membranes.

2.3.1.2. Liquid displacement method. The average pore size as well as the pore number and pore area distribution of the prepared membranes were determined by the liquid displacement method [1], also known as combined bubble pressure and solvent permeability method. In this method, the membrane is wetted previously with an appropriate penetrating liquid and then an immiscible liquid that does not wet the membrane is pressurized to pass through the pores displacing the previous liquid which is already occupying the pores. In this work, water–isobutanol–methanol (25:15:7, v/v) mixture was taken as the penetrating liquid. Deionized water was considered for the immiscible liquid. The pore size distribution was obtained from the data of variation of flow with pressure [25,26]. The following equations were used to calculate the pore size distribution:

The pore radius (r) was calculated by using the well-known Cantor's equation:

$$r = \frac{2\sigma}{P} \quad (1)$$

Where, P is the transmembrane pressure and σ is the interfacial tension between the two liquids. The total hydraulic permeability coefficient (L_n) was obtained by:

$$L_n = \sum L_{i,k} = \sum \frac{J_{i,k}}{P_{i,k}} \quad (2)$$

Where, $J_{i,k}$ is the flux at pressure $P_{i,k}$ and $L_{i,k}$ is the partial permeability coefficient of the pores with radius between r_i and r_k evaluated at $P_{i,k}$, which corresponds to a mean radius, i.e.

$$r_{i,k} = \frac{r_i + r_k}{2} \quad (3)$$

Combining Eqs. (1) and (2), flux versus pressure data gives the permeability versus pore radius curve. Again, the pore number versus pore radius and pore area versus pore radius curves can be obtained using the following equations [25,26]:

$$N_{i,k} = \frac{d\eta}{2\pi\sigma^4} P_{i,k}^3 J_{i,k} \quad (4)$$

$$A_{i,k} = \pi r_{i,k}^2 N_{i,k} \quad (5)$$

Where, $N_{i,k}$ is the pore density, i.e., the number of pores having radii between r_i and r_k per unit area of the membrane surface, d is the length of the pore which is approximately equivalent to the thickness of the skin layer and η is the viscosity of the alcohol rich mixture. $A_{i,k}$ is the area of pores having radii between r_i and r_k . Both the equations are derived from the Hagen–Poiseuille's permeation equation assuming cylindrical pores and laminar

flow. An average value of the thickness of the skin layer equal to $0.1\ \mu\text{m}$ is considered in the present work even though it is likely to vary along the surface of the membrane.

The total area A_t and the total number of pores per unit area of membrane N_t can be found as follows:

$$A_t = \sum A_{i,k} \quad (6)$$

$$N_t = \sum N_{i,k} \quad (7)$$

The mean pore radius r_m is calculated as follows [27]:

$$r_m = \frac{\sum N_{i,k} r_{i,k}}{\sum N_{i,k}} \quad (8)$$

The limitation of this method is that the absolute values of A_t , N_t and their distribution are likely to be associated with an error because of the deviation from the assumption of cylindrical pores and non-uniform thickness of membrane skin layer. However, the information may be useful in comparing the different membranes. At the same time the permeability data has got authenticity as they are obtained directly from the experiment (Eq. (2)).

2.3.2. Membrane characterization

2.3.2.1. Equilibrium water content (EWC). Equilibrium water content is considered to be an important characterization parameter as it indirectly indicates the degree of hydrophilicity or hydrophobicity of a membrane [28]. Also it is related to the porosity of a membrane. Membranes were weighed in an electronic balance in wet state after mopping the surface water with a clean tissue paper. The wet membranes were dried by putting in a vacuum oven for 24 h at a temperature of $50\text{--}60^\circ\text{C}$ and again they were weighed in dry state. Then the equilibrium water content (EWC) at room temperature is calculated as follows:

$$\text{EWC (\%)} = \frac{W_w - W_d}{W_w} \times 100 \quad (9)$$

Where, W_w is weight of wet membranes (g) and W_d is weight of dry membranes (g).

2.3.2.2. Porosity. Porosity of the membrane plays an important role on permeation and separation. The membrane porosity is determined as follows [29]:

$$\text{Porosity} = \frac{W_w - W_d}{\rho_w \times V} \quad (10)$$

Where, ρ_w is density (kg/m^3) of pure water at room temperature and V is volume of the membrane in wet state (m^3).

2.3.3. Permeation experiment

2.3.3.1. Membrane cell. The unstirred batch experiments were conducted in a 100 mL filtration cell made of Teflon. Inside the cell, a flat circular membrane was placed over a base support. The membrane diameter was $2 \times 10^{-2}\text{ m}$ and the effective area of the membrane was $3.14 \times 10^{-4}\text{ m}^2$. The permeating solution was collected from the bottom of the cell. The cell was pressurized using a nitrogen cylinder. The schematic of batch experimental set up is presented in Fig. 1.

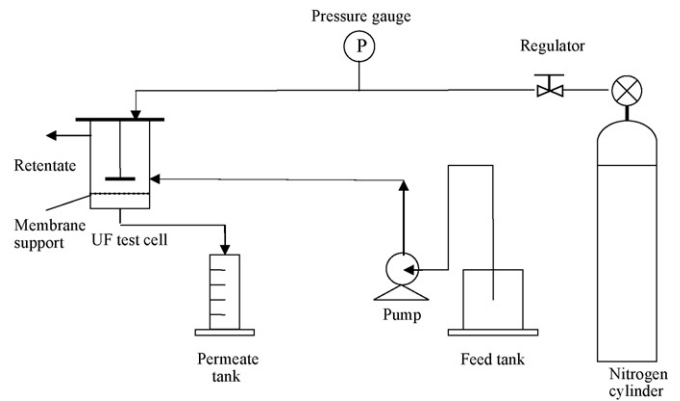


Fig. 1. Schematic diagram of the experimental set-up.

2.3.3.2. Membrane compaction. Before using each fresh membrane, it was compacted. The compaction study of each membrane was carried out with deionized water for 4 h at a transmembrane pressure of 240 kPa which is higher than the maximum operating pressure designed for the present experiments. The compact membranes were washed thoroughly before placing them in the membrane batch cell.

2.3.3.3. Hydraulic permeability (P_m) and pure water flux (PWF). Membrane hydraulic permeability has got significance particularly for membranes used in pressure-driven separation processes. Membrane permeability was determined by allowing deionized water to pass through the compact membrane. Flux values of pure water at different transmembrane pressures (ranging $0\text{--}240\text{ kPa}$) were measured under steady state condition using the following equation:

$$J_w = \frac{Q}{A \Delta T} \quad (11)$$

where J_w is pure water flux ($\text{L m}^{-2}\text{ h}^{-1}$), Q is volume of water permeated (L), A is effective membrane area (m^2) and ΔT is sampling time (h).

From the slope of the linear relationship between the pure water flux (J_w) and transmembrane pressure, hydraulic permeability was calculated as

$$P_m = \frac{J_w}{\Delta P} \quad (12)$$

Where, P_m is hydraulic permeability ($\text{L m}^{-2}\text{ h}^{-1}\text{ kPa}^{-1}$); ΔP is transmembrane pressure (kPa).

2.3.3.4. Ultrafiltration experiments. Ultrafiltration experiments were conducted in the batch cell mentioned previously to study the influence of molecular weight of PEG on solute separation and permeate flux of the membranes prepared. The protein, Bovine Serum Albumin (BSA), was dissolved in deionized water and the concentration was kept constant at 1000 mg L^{-1} for all the experiments. The pH of protein solution plays an important role in protein-membrane interaction [30,31]. The BSA solution was adjusted to different pH values with the help of buffer solutions. The pH of the BSA solution (molecular weight 68,000) was kept approximately

at two values: 4.8 (i.e. at isoelectric point) and 9.5 (i.e. at above isoelectric point). The flux was calculated using the same equation for calculating PWF, i.e. Eq. (11). Percentage rejection of BSA was calculated using the following equation:

$$R(\%) = \left(1 - \frac{C_p}{C_f}\right) \times 100 \quad (13)$$

Where, C_p and C_f are the concentration in the permeate and the feed in mg L^{-1} , respectively. Ultrafiltration tests were performed with each membrane under a transmembrane pressure of 103 kPa for BSA solutions with different pH values. The permeate was collected in a measuring cylinder over a constant time interval for calculating flux. Duration of each experiment was 1 h. Later the BSA concentration in the permeate was determined spectrophotometrically using a UV–vis spectrophotometer (Perkin–Elmer Precisel, Lambda-35) at a wavelength of 280 nm. The main objective of the ultrafiltration experiment was

to investigate the rejection behaviour of BSA protein by different membranes prepared in the present work under identical conditions. After thoroughly cleaning the system several times by distilled water, the membrane permeability was re-evaluated with pure water. It was observed that the membrane permeability remained almost constant between successive runs.

3. Results and discussion

3.1. Morphological study

Microscopic study through SEM analysis is carried out to have qualitative information regarding surface and cross-sectional morphology of the membranes prepared. The liquid displacement method is adopted to have quantitative information with respect to membrane morphology such as pore size, pore number, pore area and pore permeability.

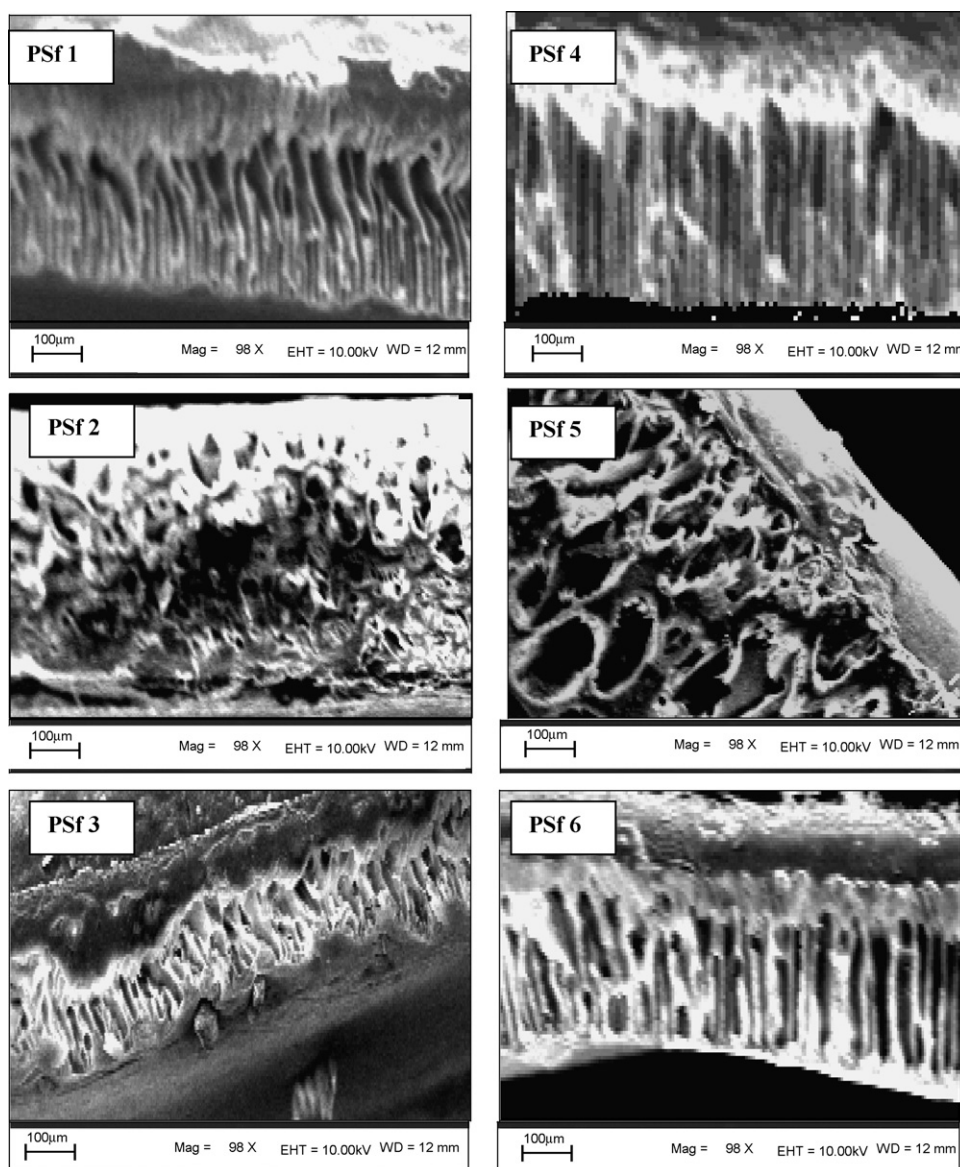


Fig. 2. Cross-sectional SEM images for different membranes.

3.1.1. SEM analysis

SEM analysis is an important technique for microscopic observations of the membrane morphology. Fig. 2 showed the SEM image of the cross-section of different membranes. The effect of different molecular weight of additive (PEG) as well as two different solvents (NMP and DMAc) is shown in the figure. It may be seen from the figure that membranes so formed are having asymmetric structure consisting of a dense top layer and a porous sub layer. The sublayer seems to have finger-like cavities as well as macrovoid structure. Similar observations were also found by Strathmann et al. [32] for the systems of polyamide as the polymer using dimethylsulfoxide (DMSO), DMF, DMAc and NMP as solvents, separately with LiCl as the additive. Due to high mutual affinity of NMP and DMAc for water, instantaneous demixing results, leading to the formation of finger like cavities in the sublayer of the prepared membranes [1]. It may also be seen from the figure that the addition of PEG of different molecular weight for both type of solvents causes

significant suppression of the finger-like cavities in the sublayer. These observations lead to the inference that though instantaneous demixing is still maintained, the molecular weight of PEG might have substantial role on the precipitation rate [1,32,33].

SEM images for the top surface (air side) of different membranes are presented in Fig. 3. The reason for such type of surface morphology may be explained from the concept of quaternary phase diagram of membrane formation. The formation of the top surface is possibly due to demixing of the casting solution by means of nucleation and growth of the polymer rich phase, i.e. the solid phase [34,35]. This results in nodule/aggregate formation on the surface that leads to much better interconnected pores. With increase in molecular weight of PEG, the nodular structure of the membrane top layer becomes more prominent. It may be attributed to the result of spinodal demixing which according to Boom et al. [4], is likely to occur for systems with high molecular weight additives because of their lower mobility in the initial stage of immersion in the coagulation bath.

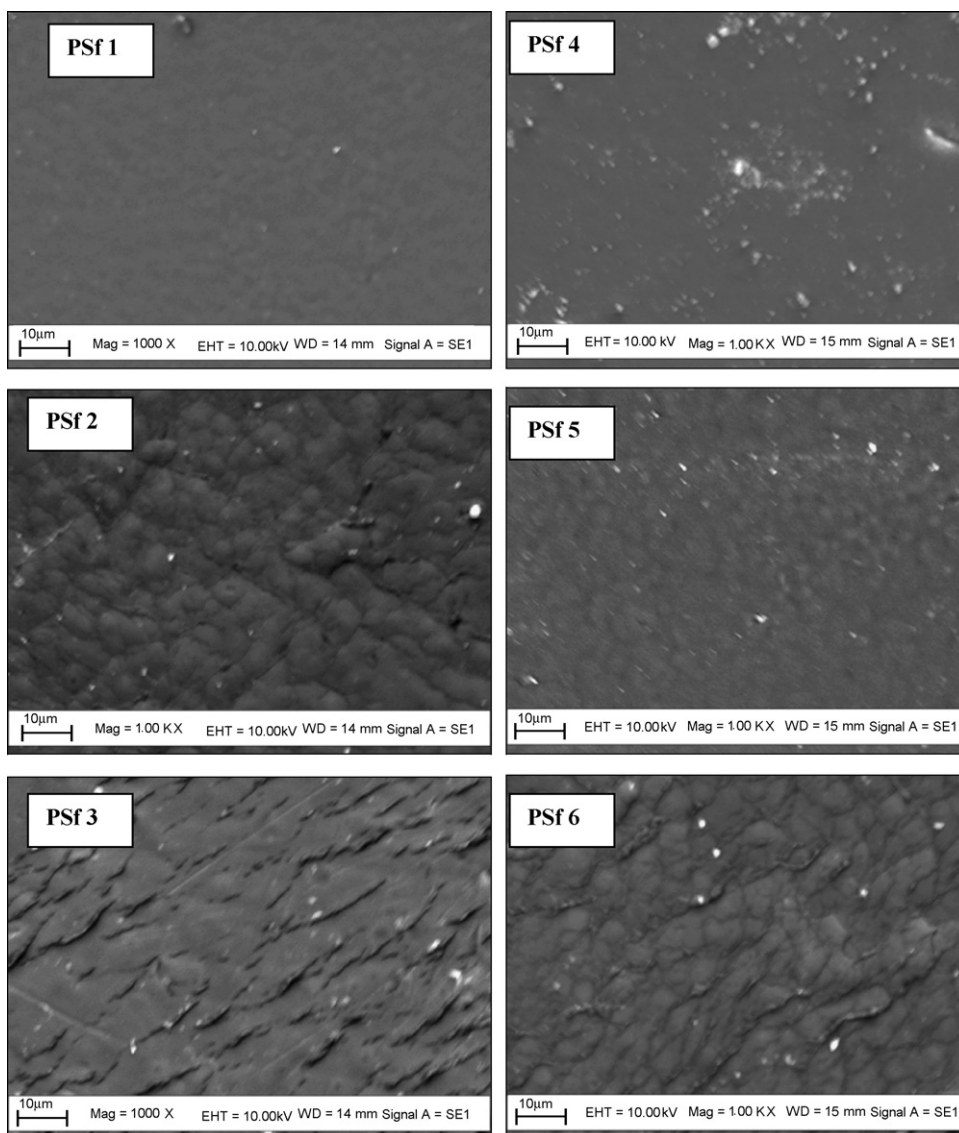


Fig. 3. SEM images of top surface (air-side) of different membranes.

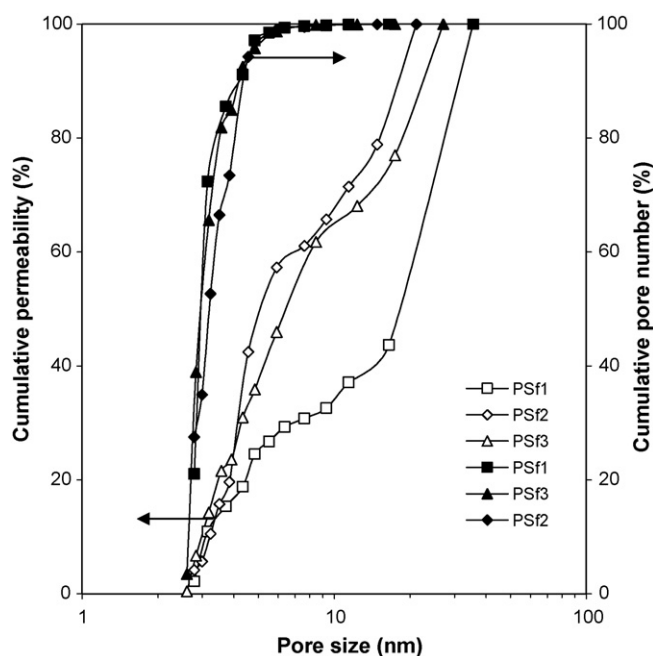


Fig. 4. Variation of cumulative permeability (%) and cumulative pore number (%) with pore size for PSf1, PSf2 and PSf3 membranes.

3.1.2. Liquid displacement studies

This method helps us to evaluate the transmembrane pores of the membranes in wet state i.e. under the condition similar to that of ultrafiltration operation. The membrane pore permeability, pore number and pore area for each membrane were determined using Eqs. (2), (4) and (5). Membrane permeability and pore number are plotted against pore radius as cumulative curves and presented in Figs. 4 and 5 for both the systems (i.e. PSf/NMP/PEG and PSf/DMAc/PEG). From the figures it is observed that majority of the pores (approx. 80%) are in the 2–5 nm range. However, the exact fraction of the larger pores (>100 nm) as well as smaller pores (<2 nm) cannot be determined due to the pressure limitation of the experimental set-up. For all the membranes, though the majority of pores (approx. 80%) are having a radius in the range of 2–5 nm, these pores contribute not more than 20% to the overall permeability. The small number of larger pores actually determines the overall membrane performance by increasing the overall permeability. Similar type of result was observed by Munari et al. [26] with PVDF/PVP system. This fact can be explained from the Hagen–Poissuille equation which says that transport through membranes (i.e. permeability) is directly proportional to the fourth power of pore radius.

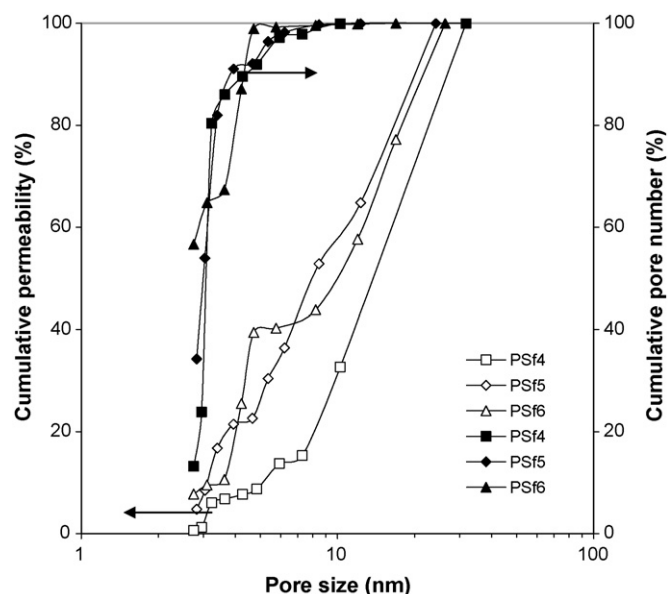


Fig. 5. Variation of cumulative permeability (%) and cumulative pore number (%) with pore size for PSf4, PSf5 and PSf6 membranes.

Table 2 reports the results of liquid displacement method. It is seen that for both type of solvents, with increase in molecular weight of PEG, the pore number of all the membranes increases resulting in more porous membranes. The pore number per unit area (N_l) for PSf/NMP/PEG system is found to increase from 5.8×10^8 to 2.1×10^9 , while for PSf/DMAc/PEG system it is from 4.8×10^8 to 2.2×10^9 . The total hydraulic permeability coefficient (L_n) is also affected by the molecular weight of PEG. For PSf/NMP/PEG membranes, the value of L_n is found to be 0.004 m/s MPa for PEG 400, 0.003 m/s MPa for PEG 6000 and 0.009 m/s MPa for PEG 20000 while for PSf/DMAc/PEG system, the value of L_n is found to be 0.007 m/s MPa for PEG 400, 0.006 m/s MPa for PEG 6000 and 0.01 m/s MPa for PEG 20000. However, the average pore size (calculated from Eq. (8)) is found to be not much affected by the molecular weight of PEG though it is marginally decreasing. This decreasing trend may be attributed to the difference in diffusion rates of different molecular weight of PEG. When the casting solution comes into contact with the nonsolvent in the coagulation bath, there is a rapid outflow of the solvent from the casting solution to the coagulation bath causing the higher concentration polymer molecules to aggregate at the top layer [36]. Smaller molecular weight additives having comparatively higher diffusivity rates can diffuse out during immersion along with the solvent. In contrast to that, the diffusion rates of higher molecular weight

Table 2
Morphological parameters of all membranes obtained from liquid displacement method

Membranes	PSf1	PSf2	PSf3	PSf4	PSf5	PSf6
r_{av} (nm)	3.44	3.44	3.42	3.57	3.43	3.39
L_n (m/s MPa)	4×10^{-3}	3×10^{-3}	9×10^{-3}	7×10^{-3}	6×10^{-3}	1×10^{-2}
ΣN_i (cm ²)	5.8×10^8	6.6×10^8	2.1×10^9	4.8×10^8	1.2×10^9	2.2×10^9
ΣA_i (cm ²)	2.3×10^{-4}	3.0×10^{-4}	8.5×10^{-4}	2.3×10^{-4}	4.9×10^{-4}	8.7×10^{-4}

additives (PEG 20000) are much lower than the solvent and so according to Idris et al. [37] they take more time to reach the surface. This will give sufficient time for the polymer molecules to aggregate on top of it and form a denser top layer with relatively smaller size pores. So it may be inferred that PEG acts both as a pore former and pore size reducer in membrane formation and with increase in molecular weight, its capacity to form pores increases.

3.2. Membrane characterization by the determination of equilibrium water content (EWC) and porosity

3.2.1. Effect of molecular weight of PEG on EWC

EWC is an important parameter for membrane characterization as it is closely related to PWF. The equilibrium water content of different membranes is presented in Table 3. It may be found from the table that increase of molecular weight of PEG increases the EWC of all membranes. Again, for higher molecular weight of PEG (i.e. 20000), the EWC for PSf/NMP membranes are higher than PSf/DMAc membranes and for molecular weight of PEG (up to 6000), the EWC for PSf/DMAc membranes are marginally higher than PSf/NMP membranes. These may be attributed to the higher or lower porosities in the respective cases (Table 3).

From Table 3, it is observed that for PSf/NMP/PEG membranes, the EWC for PEG 400 is 56.8%, for PEG 6000 is 68.2% and for PEG 20000 is 78.8%. Similar trend is seen for PSf/DMAc/PEG membranes, where for PEG 400 it is 58.6%, for PEG 6000 it is 69.1% and for PEG 20000 it is 76.4%. This increasing trend confirms the presence of increasing number of pores in the membrane with the increase of molecular weight of PEG (as discussed in Section 3.1). The pores on the surface as well as cavities in the sublayer are responsible for accommodating water molecules in the membranes [38].

3.2.2. Effect of molecular weight of PEG on membrane porosity

The porosity of each membrane is calculated using Eq. (10) and are reported in Table 3. It is observed that porosity is almost independent of type solvent used in the present work. However, two different findings are observed with molecular weights of PEG. Firstly, porosity of the membranes remains almost unchanged up to the molecular weight of 6000. Secondly, a significant increase in porosity is found when molecular weight of PEG increases from 6000 Da to 20,000 Da.

Table 3 shows that porosity of all membranes remains in between 0.38 and 0.39 when molecular weight of PEG remains within 6000. Porosity increases to 0.58–0.59 when molecular weight of PEG increases to 20000 for both the solvent system.

The variation of porosity may be explained on the basis of thermodynamic and kinetic consideration. Addition of an additive into the casting solution has two effects. Firstly, it causes thermodynamic enhancement of the phase separation by reducing the miscibility of the casting solution with the nonsolvent; this results in instantaneous demixing. Secondly, it causes kinetic hindrance against phase separation by increasing the viscosity of the solution; this results in delayed demixing [1,32,34]. Increase in viscosity increases the ratio of non-solvent inflow to solvent outflow which according to the theory suggested by Young et al. [39] results in a more porous membrane. Thus, the increase in porosity in membranes with PEG 20000 may be due to decrease in miscibility of the casting solution with water with addition of PEG 20000. This in turn, can work in favour of the thermodynamic enhancement in the demixing of casting solution.

3.3. Permeation experiments

Membranes that have been prepared separately with NMP and DMAc as solvents are tested to see the effect of addition of PEG of different molecular weight on their permeation behaviour. The membranes are characterized in terms of PWF, hydraulic permeability and rejection as well as permeate flux behaviour of protein at different pH.

3.3.1. Flux profile during compaction

All the membranes are subjected to hydraulic compaction at a constant transmembrane pressure of 240 kPa. The compaction is carried out for 4 h until a steady-state flux is attained. The water flux is calculated using Eq. (11) from the experimental permeate flow rate measured at every 30 min interval.

The effect of compaction time on PWF for all the membranes is shown in Figs. 6 and 7 for NMP and DMAc, respectively. It is seen that the PWF declines gradually due to compaction with time and after about 2 h of compaction, it reaches a steady-state value. This is due to the fact that the walls of the pores become closer, denser and uniform resulting in reduction in pore size as well as the flux during compaction [1].

The steady-state value of PWF for each membrane corresponding to the applied pressure (240 kPa) is found to increase with molecular weight of PEG for both the solvents. The steady state flux increases from 21.0 L/m² h to 4051 L/m² h for PSf/NMP/PEG membranes and from 33.6 L/m² h to 964.6 L/m² h for PSf/DMAc/PEG system, when molecular weight of PEG increases from 400 to 20000. The increase in flux with increase in molecular weight of PEG is due to the increase in porosity as discussed in the preceding section.

Table 3
Values of some characterization parameters of all membranes

Membranes	PSf1	PSf2	PSf3	PSf4	PSf5	PSf6
Water content (%)	56.8	68.2	78.8	58.6	69.1	76.4
Porosity	0.38	0.38	0.59	0.39	0.39	0.58
Hydraulic permeability (L m ⁻² h ⁻¹ kPa ⁻¹)	0.094	2.2	17.6	0.14	2.5	3.66

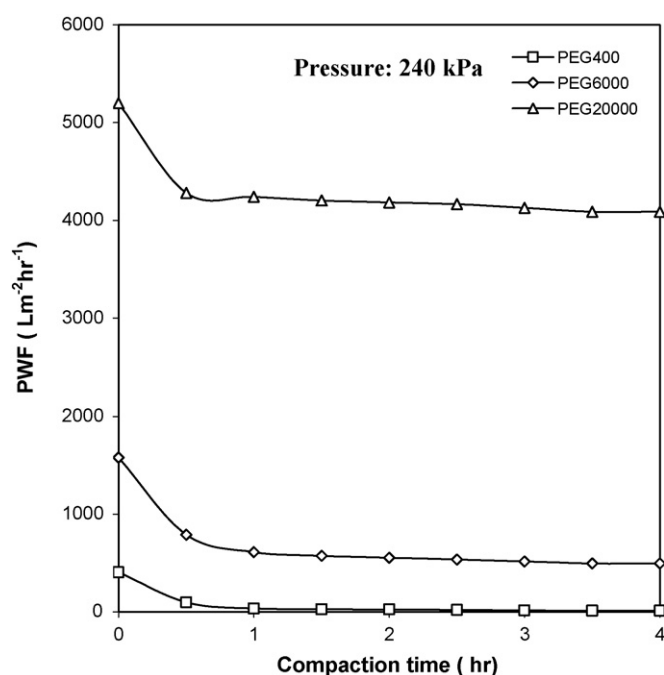


Fig. 6. Flux profile during compaction for PSf/NMP/PEG membranes.

Again the higher values of PWF for PSf/NMP/PEG membranes for higher molecular weight of PEG (i.e. PEG 20000) compared to PSf/DMAc/PEG membranes are possibly due to relatively higher porosity of the former membrane. This result agrees to the findings of the EWC test (Table 3).

3.3.2. Effect of molecular weight of PEG on PWF and hydraulic permeability (P_m)

PWF as well as hydraulic permeability is considered to be the key specification factors for any membrane.

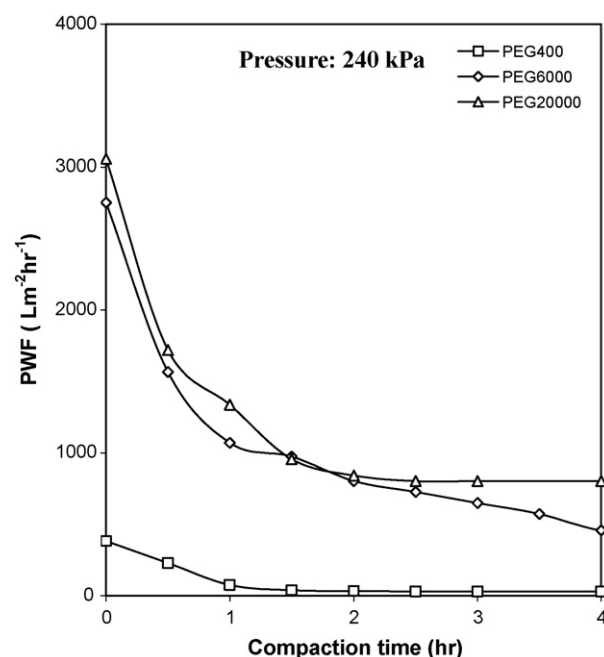


Fig. 7. Flux profile during compaction for PSf/DMAc/PEG membranes.

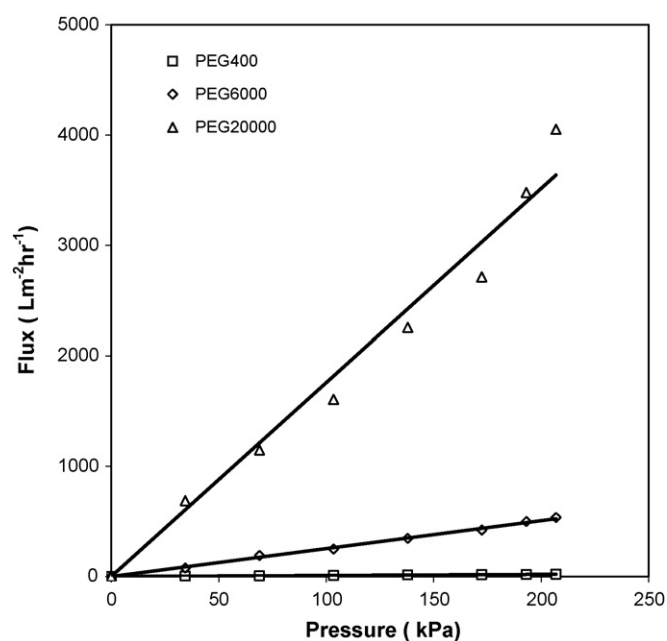


Fig. 8. Effect of transmembrane pressure on PWF for PSf/NMP/PEG membranes.

The effect of molecular weight of PEG on PWF at various transmembrane pressures is shown in the Figs. 8 and 9. It is seen that within the range of 0–240 kPa, with increase in transmembrane pressure, PWF increases almost linearly for all the membranes. This is due to the increase in effective driving force (transmembrane pressure) required for water permeation. The PWF is also seen to increase with increase in molecular weight of PEG at a particular pressure irrespective of the solvent used which agrees with the findings of the compaction

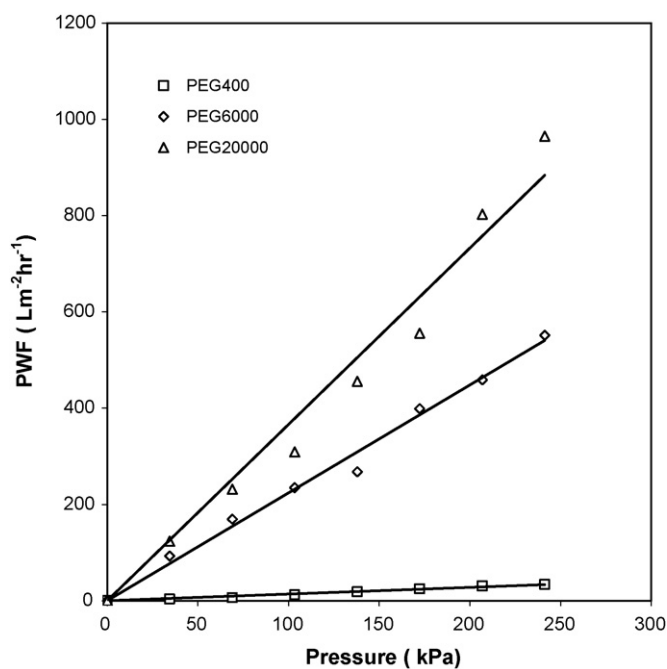


Fig. 9. Effect of transmembrane pressure on PWF for PSf/DMAc/PEG membranes.

study. For example, at 173 kPa, The PWF increases from 15.3 to 2713.4 $\text{L m}^{-2} \text{h}^{-1}$ and from 24.5 to 555.6 $\text{L m}^{-2} \text{h}^{-1}$ for PSf/NMP and PSf/DMAc systems, respectively, when molecular weight of PEG increases from 400 to 20000.

Permeability is determined from the slope of the plots in Figs. 8 and 9 using Eq. (12) and is represented in Table 3. It is observed that hydraulic permeability (P_m) increases with the molecular weight of PEG. P_m for PSf/NMP/PEG membranes increases from 0.094 to 17.6 ($\text{L m}^{-2} \text{h}^{-1} \text{kPa}^{-1}$) and for PSf/DMAc/PEG membranes it increases from 0.14 to 3.66 ($\text{L m}^{-2} \text{h}^{-1} \text{kPa}^{-1}$) when molecular weight of PEG increases from 400 to 20000. Again the higher permeability of PSf/NMP membranes compared to PSf/DMAc membranes with high molecular weight PEG confirms the finding of the compaction study that porosity of PSf/NMP membranes is more than that of PSf/DMAc membranes for PEG 20000.

The result clearly indicates that addition of PEG with different molecular weights influence the formation of pores in the membranes, which affect the permeability as the latter is conceptually related to its pores for UF membranes [6,40]. According to Refs. [5,41] removal of additives completely from the membrane matrix becomes more and more difficult as the molecular weight of additives such as PEG and PVP goes on increasing. Therefore, the residual additives, which are hydrophilic in nature, are compelled to stay inside the matrix permanently, thus, making the membrane more hydrophilic [5,8,41,42]. It is also reported by Chou et al. [43] in their study with PEG and cellulose acetate that PEG is entangled with the membrane matrix leading to its stable existence in the matrix. In the present study it is possible that due to very high molecular weight of hydrophilic PEG (20000 Da), trace amount of PEG may always remain entrapped in the membrane matrix. This in turn can change the hydrophobic behaviour of Polysulfone membrane to hydrophilic behaviour. Thus, in addition to porosity, increase in hydrophilicity with increase in molecular weight of PEG may be another important factor to describe such performances of the prepared membranes. However, this can be confirmed only after thorough investigation of the existence of the PEG in the membrane surface layer particularly during addition of PEG 20000.

3.3.3. Variation of permeate flux and BSA rejection during permeation experiments

Apart from transmembrane pressure, the rejection and flux characteristics of the membrane strongly depend on the structure of the membrane as well as the properties of the feed solution. So, the synthesized UF membranes were also characterized by estimating rejection and flux during permeation experiment with BSA solution as feed.

The variation of permeate flux and BSA rejection data with different molecular weight of PEG are shown in Figs. 10 and 11 for NMP and DMAc solvent, respectively at pH 4.8 (i.e. at isoelectric point) and at pH 9.5 (i.e. above isoelectric point) conditions. From these figures, it is understood that both molecular weight of PEG and pH of the protein solution are important factors in protein rejection and flux.

The flux and rejection of proteins by ultrafiltration membranes can be explained under the concept of protein adsorption

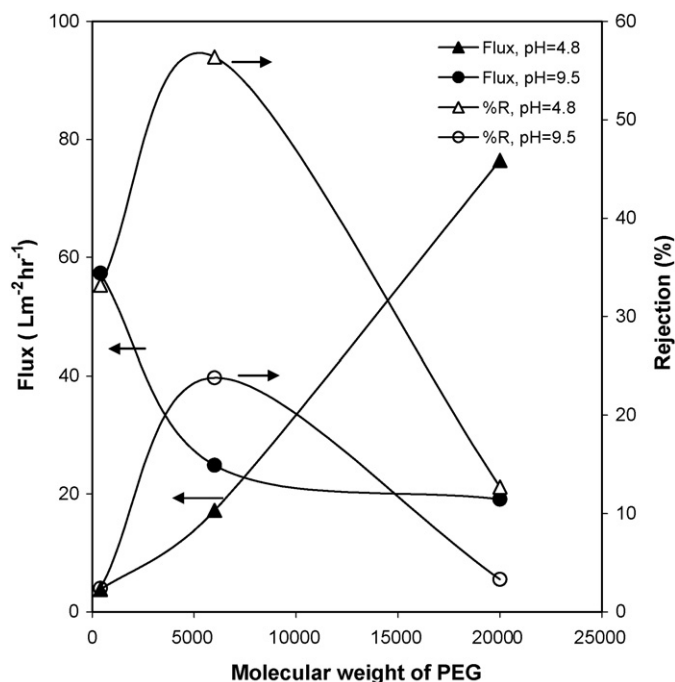


Fig. 10. Effect of different molecular weight of PEG and pH of BSA solution on permeate flux and rejection; membranes used: PSf1, PSf2 and PSf3; pressure: 103 kPa; operating time: 1 h.

and consequent pore narrowing, as a result of both hydrophobic and electrostatic interactions between the membrane surface and the protein molecules [30]. The morphological structure of the membrane (which includes both top-layer and sublayer) in protein transmission or rejection also play an important role.

When the pH of the BSA solution is maintained near the isoelectric point (i.e. pH 4.8), it is observed that the flux grad-

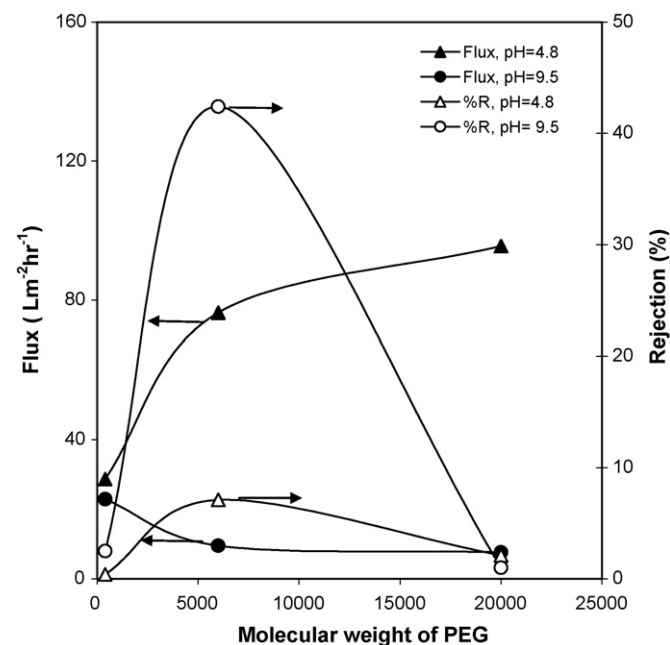


Fig. 11. Effect of different molecular weight of PEG and pH of BSA solution on permeate flux and rejection; membranes used: PSf4, PSf5 and PSf6; pressure: 103 kPa; operating time: 1 h.

usually increases with increase in molecular weight of PEG from 400 Da to 20000 Da for all membranes, irrespective of the solvents; This effect can be seen in Figs. 10 and 11. As protein carries no charge at its isoelectric point, this trend may be due to the result of hydrophobic/hydrophilic interaction between the protein molecules and the membranes. In general, hydrophilic membranes tend to adsorb less protein at its isoelectric point and thus have higher flux than hydrophobic membranes [44]. This is because of the fact that less adsorption does not narrow down the pores. In the present study, increase in porosity of the membranes (from water content test) and possible increase in hydrophilicity as discussed earlier with increase in molecular weight of PEG, leads to increase in flux. On the other hand, from both the figures, it is seen that percent rejection of BSA increases with increase in molecular weight of PEG from 400 Da to 6000 Da. The increasing trend in percentage rejection with increase in molecular weight of PEG from 400 Da to 6000 Da may be because of the resistance offered by the dense and sponge-like structure of the membranes (Fig. 2) with PEG 6000 to the protein molecules. It is also found that rejection decreases beyond molecular weight of PEG 6000 Da. At pH 4.8, in absence of electrostatic interaction, protein transmission should increase i.e. rejection should decrease with increase in molecular weight of PEG. The increase in membrane porosity (Table 3) as well as presence of finger-like cavities in the sub-layer (Fig. 2) and possible increase in hydrophilicity with PEG 20000 allow more protein transmission without much adsorption and consequently result in less rejection.

When the pH of the solution is kept at 9.5, the flux shows an opposite trend i.e. it gradually decreases with increase in molecular weight of PEG. In this case, adsorptive effects through electrostatic interactions between protein and membrane surfaces may become more pronounced. This may be due to the fact that above isoelectric point (i.e. pH 9.5), protein carries a net negative charge [45] resulting in attractive interactions between protein molecules and membranes. This interaction increases for membranes with higher molecular weight PEG possibly because of their higher hydrophilicity. So flux decreases as adsorption of protein on pore wall causes pore narrowing. The trend of percent rejection is similar to that at pH 4.8. Apparently, it appears that the rejection should increase with increase in adsorption of protein as molecular weight of PEG increases. But experimental result is seen to be just reverse for PEG 20000 membranes. The reason for PEG 20000 membranes having minimum rejection may be because of the fact that adsorption of protein on pore wall has less effect on pore narrowing due to their very high porosity compared to PEG 400 and PEG 6000.

The high rejection and comparatively low flux with PEG 6000 membranes for both the pH values may also be understood from the morphology of their cross section [as discussed in Section 3.1]. The thin asymmetric layer probably explains for the improvement in the rejection rate while the thick sponge-like sub layer offers resistance resulting in rather low flux and high rejection.

The role of solvent in the casting solution on rejection of proteins can also be noted from the figures. It is seen that for NMP, the percentage rejection is found to be maximum at pH value of

4.8 which is 56.4 percent for PEG 6000; while for DMAc, it is maximum for pH value of 9.5 which is 42.4% for PEG 6000. This may be attributed to the fact that at pH value of 4.8, adsorption of protein, taking place due to hydrophobic/hydrophilic interaction between the protein molecules and the membranes, on NMP membrane is possibly more than on DMAc membrane resulting in higher rejection (56.4%). On the other hand, at pH value of 9.5, adsorption of protein, taking place due to the electrostatic attraction between the protein molecule and the membrane surface, is possibly more in DMAc membranes leading to higher rejection (42.4%) compared to NMP membranes.

Thus from the above discussion, it may be concluded that the hydrophobic or electrostatic interaction between protein molecules and membrane surface depending on the range of pH of protein solution determines the extent of protein rejection by a membrane. The morphological parameters of a membrane (such as porosity) and structure of membrane (with finger-like or spongy-like sub layer) also play a key role in this regard. Lastly, effect of molecular weight of additives (i.e. PEG) and type of solvents (i.e. NMP and DMAc) may also be considered as important factors as they finally decide the morphology and property of a membrane.

4. Conclusion

Flat sheet PSf membranes were prepared from casting solutions containing 12 wt% of PSf with two different solvents, viz. NMP and DMAc, separately, using diffusion induced phase separation process. PEG of average molecular weights of 400 Da, 6000 Da and 20000 Da were used as additive. Effects of molecular weight of PEG on the morphology such as porosity in terms of average pore size, pore number distribution and pore area distribution were studied in detail. The permeation performance of the prepared membranes with varying molecular weight of PEG was also evaluated in terms of PWF, hydraulic permeability and rejection efficiency of BSA protein. The observations can be summarized as follows:

- All the membranes were found to have asymmetric structure as seen from SEM photographs.
- PEG 6000 can be a suitable additive for making asymmetric membranes having a dense skin layer and a relatively macrovoid-free sponge-type support layer.
- With increase in molecular weight of PEG, the pore number as well as pore area per unit surface area (porosity) of the prepared membrane was increased. However, the average pore size was seen to reduce marginally. So, PEG could be regarded as a pore former agent rather than pore reducing agent.
- The PWF and hydraulic permeability were seen to enhance greatly with increase in molecular weight of PEG.
- A significant increase in rejection was observed in BSA separation when molecular weight of PEG was increased from 400 Da to 6000 Da in the membrane casting solution. Beyond that the rejection decreases. The pH of the protein solution also seems to play an important role in this regard. Irrespective of the solvents and pH of the protein solutions, the membranes with PEG 6000 as additive seems to exhibit the highest solute

separation. The maximum separation was only 56.4% with PSf2 membranes when the pH of the protein solution was kept near its isoelectric point which indicates that the given composition for the prepared membranes may not be recommended for efficient protein separation. However, a detail parametric investigation (i.e. effect of pressure, BSA concentration and stirring) is required to find out the optimum condition for the better rejection performance.

References

- [1] M. Mulder, Basic Principles of Membrane Technology, Kluwer Academic Publishers, Dordrecht, 1991.
- [2] S. Munari, A. Botino, G. Camera Roda, G. Capannelli, Preparation of ultrafiltration membranes. State of the art, *Desalination* 77 (1990) 85–100.
- [3] A.J. Reuvers, J.W.A. van den Berg, C.A. Smolders, Formation of membranes by means of immersion precipitation. Part IA. Model to describe mass transfer during immersion precipitation, *J. Membr. Sci.* 34 (1987) 45–65.
- [4] R.M. Boom, I.M. Wienk, Th. Van den Boomgaard, C.A. Smolders, Microstructures in phase inversion membranes. Part 2. The role of a polymeric additive, *J. Membr. Sci.* 73 (1992) 277–292.
- [5] I.M. Wienk, R.M. Boom, M.A.M. Beerlage, A.M.W. Bulte, C.A. Smolders, Recent advances in the formation of phase inversion membranes made from amorphous or semi-crystalline polymers, *J. Membr. Sci.* 113 (1996) 361–371.
- [6] D.B. Mosqueda-Jimenez, R.M. Narbaitz, T. Matsuura, G. Chowdhury, G. Pleizier, J.P. Santerre, Influence of processing conditions on the properties of ultrafiltration membranes, *J. Membr. Sci.* 231 (2004) 209–224.
- [7] H.T. Yeo, S.T. Lee, M.J. Han, Role of polymer additive in casting solution in preparation of phase inversion polysulfone membranes, *J. Chem. Eng. Japan* 33 (2000) 180–185.
- [8] B. Jung, J.K. Yoon, B. Kim, H.W. Rhee, Effect of molecular weight of polymeric additives on formation, permeation properties and hypochlorite treatment of asymmetric polyacrylonitrile membranes, *J. Membr. Sci.* 243 (2004) 45–57.
- [9] M.J. Han, S.T. Nam, Thermodynamic and rheological variation in polysulfone solution by PVP and its effect in the preparation of phase inversion membrane, *J. Membr. Sci.* 202 (2002) 55–61.
- [10] M.J. Han, Effect of propionic acid in the casting solution on the characteristics of phase inversion polysulfone membranes, *Desalination* 121 (1999) 31–39.
- [11] T.P. Hou, S.H. Dong, L.Y. Zheng, The study of mechanism of organic additives action in the polysulfone membrane casting solution, *Desalination* 83 (1991) 343–360.
- [12] Q.Z. Zheng, P. Wang, Y.N. Yang, Rheological and thermodynamic variation in polysulfone solution by PEG introduction and its effect on kinetics of membrane formation via phase-inversion process, *J. Membr. Sci.* 279 (2006) 230–237.
- [13] S. Deniz, Characteristics of polycarbonate membranes with polyethylene glycol prepared via dry/wet-phase inversion methods, *Desalination* 200 (2006) 42–43.
- [14] B.K. Chaturvedi, A.K. Ghosh, V. Ramachandran, M.K. Trivedi, M.S. Hanra, B.M. Misra, Preparation, characterization and performance of polyethersulfone ultrafiltration membranes, *Desalination* 133 (2001) 31–40.
- [15] B.T. Sanchez, R.I. Ortiz-Basurto, E.B. Fuente, Effect of nonsolvents on properties of spinning solutions and polyethersulfone hollow fiber ultrafiltration membranes, *J. Membr. Sci.* 152 (1999) 19–28.
- [16] N.A. Ochoa, P. Pradanos, L. Palacio, C. Pagliero, J. Marchese, A. Hernandez, Pore size distributions based on AFM imaging and retention of multidisperse polymer solutes: Characterisation of polyethersulfone UF membranes with dopes containing different PVP, *J. Membr. Sci.* 187 (2001) 227–237.
- [17] J.J. Qin, M.H. Oo, Y. Li, Development of high flux polyethersulfone hollow fiber ultrafiltration membranes from a low critical solution temperature dope via hypochlorite treatment, *J. Membr. Sci.* 247 (2004) 137–142.
- [18] I.C. Kim, K.H. Lee, Effect of poly(ethylene glycol) 200 on the formation of a polyetherimide asymmetric membrane and its performance in aqueous solvent mixture permeation, *J. Membr. Sci.* 230 (2004) 183–188.
- [19] J.H. Kim, K.H. Lee, Effect of PEG additive on membrane formation by phase inversion, *J. Membr. Sci.* 138 (1998) 153–163.
- [20] J.J. Shieh, T.S. Chung, R. Wang, M.P. Srinivasan, D.R. Paul, Gas separation performance of poly(4-vinylpyridine)/polyetherimide composite hollow fibers, *J. Membr. Sci.* 182 (2001) 111–123.
- [21] A. Idris, N.M. Zain, M.Y. Noordin, Synthesis, characterization and performance of asymmetric polyethersulfone (PES) ultrafiltration membranes with polyethylene glycol of different molecular weights as additives, *Desalination* 207 (2007) 324–339.
- [22] H. Kamusewitz, M. Schossig-Tiedemann, M. Keller, D. Paul, Characterization of polymeric membranes by means of scanning force microscopy (SFM) in comparison to results of scanning electron microscopy (SEM), *Surf. Sci.* 377–379 (1997) 1076–1081.
- [23] L. Palacio, P. Pradanos, J.I. Calvo, A. Hernandez, Porosity measurements by a gas penetration method and other techniques applied to membrane characterization, *Thin Solid Films* 348 (1999) 22–29.
- [24] K.J. Kim, A.G. Fane, C.J.D. Fell, T. Suzuki, M.R. Dickson, Quantitative microscopic study of surface characterization of ultrafiltration membranes, *J. Membr. Sci.* 54 (1990) 89–102.
- [25] P. Abaticchio, A. Bottino, G. Capannelli, S. Munari, Characterization of ultrafiltration polymeric membranes, *Desalination* 78 (1990) 235–255.
- [26] S. Munari, A. Bottino, G. Capannelli, P. Moretti, Membrane morphology and transport properties, *Desalination* 53 (1985) 11–23.
- [27] G. Capannelli, F. Vigo, S. Munari, Ultrafiltration membranes-characterization methods, *J. Membr. Sci.* 15 (1983) 289–313.
- [28] G. Arthanareeswaran, C.S. Latha, D. Mohan, M. Raajenthiren, K. Srinivasan, Studies on cellulose acetate/low cyclic dimmer polysulfone blend ultrafiltration membranes and their application, *Sep. Sci. Technol.* 41 (2006) 2895–2912.
- [29] Z. Chen, M. Deng, Y. Chen, G. He, M. Wu, J. Wang, Preparation and performance of cellulose acetate/polyethyleneimine blend microfiltration membranes and their applications, *J. Membr. Sci.* 235 (2004) 73–86.
- [30] D.A. Musale, S.S. Kulkarni, Relative rates of protein transmission through poly(acrylonitrile) based ultrafiltration membranes, *J. Membr. Sci.* 136 (1997) 13–23.
- [31] A. Higuchi, Y. Ishida, T. Nakagawa, Surface modified polysulfone membranes separation of mixed proteins and optical resolution of tryptophan, *Desalination* 90 (1993) 127–136.
- [32] H. Strathmann, K. Kock, P. Amar, R.W. Baker, The formation mechanism of asymmetric membranes, *Desalination* 16 (1975) 179–203.
- [33] R. Malaisamy, D.R. Mohan, M. Rajendran, Polyurethane and sulfonated polysulfone blend ultrafiltration membranes, *J. Colloid Interface Sci.* 254 (2002) 129–140.
- [34] A.J. Reuvers, C.A. Smolders, Formation of membranes by means of immersion precipitation. Part II, The mechanism of formation of membranes prepared from the system cellulose acetate–acetone–water, *J. Membr. Sci.* 34 (1987) 67–86.
- [35] K. Kimmerle, H. Strathmann, Analysis of the structure-determining process of phase inversion membranes, *Desalination* 79 (1990) 283–302.
- [36] W.Y. Chuang, T.H. Young, W.Y. Chiu, C.Y. Lin, The effect of polymeric additives on the structure and permeability of poly(vinyl alcohol) asymmetric membranes, *Polymer* 41 (2002) 5633–5641.
- [37] A. Idris, L.K. Yet, The effect of different molecular weight PEG additives on cellulose acetate asymmetric dialysis membrane performance, *J. Membr. Sci.* 280 (2006) 920–927.
- [38] M. Sivakumar, R. Malaisamy, C.J. Sajitha, D. Mohan, V. Mohan, R. Rangarajan, Ultrafiltration application of cellulose acetate–polyurethane blend membranes, *Euro. Polym. J.* 35 (1999) 1647–1651.
- [39] T.H. Young, L.W. Chen, A diffusion-controlled model for wet casting membrane formation, *J. Membr. Sci.* 59 (1991) 169–181.

- [40] A.G. Fane, C.J.D. Fell, A.G. Waters, The relationship between membrane surface pore characteristics and flux for ultrafiltration membranes, *J. Membr. Sci.* 9 (1981) 245–262.
- [41] C. Feng, R. Wang, B. Shi, G. Li, Y. Wu, Factors affecting pore structure and performance of poly(vinylidene fluoride-co-hexafluoro propylene) asymmetric porous membrane, *J. Membr. Sci.*, 277 (1–2) (2006) 55–64.
- [42] J. Marchese, M. Ponce, N.A. Ochoa, P. Pradanos, L. Palacio, A. Hernandez, Fouling behaviour of polyethersulfone UF membranes made with different PVP, *J. Membr. Sci.* 211 (2003) 1–11.
- [43] W.L. Chou, D.G. Yu, M.C. Yang, C.H. Jou, Effect of molecular weight and concentration of PEG additives on morphology and permeation performance of cellulose acetate hollow fibers, *Sep. Purif. Technol.* 57 (2007) 207–217.
- [44] E. Matthiasson, The role of macromolecular adsorption in fouling of ultrafiltration membranes, *J. Membr. Sci.* 16 (1983) 23–36.
- [45] D.A. Mussale, S.S. Kulkarni, Fouling reduction in poly(acrylonitrile-co-acrylamide) ultrafiltration membranes, *J. Membr. Sci.* 111 (1996) 49–56.